

DELAYED NEUTRON EMISSION MEASUREMENTS FROM FAST FISSION OF U-235 AND NP-237

William S. Charlton^a, Theodore A. Parish^a, Subramanian Raman^b,
Nubuo Shinohara^c, and Masaki Andoh^c

RECEIVED

SEP 19 1996

OSTI

^aTexas A&M University, College Station, TX 77843-3133, USA (E-mail:
charlton@trinity.tamu.edu or tap@trinity.tamu.edu)

^bOak Ridge National Laboratory, P. O. Box 2008, Oak Ridge, TN 37831-6354, USA

^cJapan Atomic Energy Research Institute, Tokai-mura, Ibaraki-ken 319-11, JAPAN

ABSTRACT

Experiments have been designed and conducted to measure the periods and yields of delayed neutrons from fast fission of U-235 and Np-237. These measurements were performed in a pool type reactor using a fast flux in-core irradiation device. The energy-dependent neutron flux spectrum within the irradiation device was characterized using a foil activation technique and the SAND-II unfolding code. Five delayed neutron groups were measured. The total yield (sum of the five group yields) for U-235 was found to be 0.0141 ± 0.0009 . The total yield for Np-237 was found to be 0.0102 ± 0.0008 . The total delayed neutron yield data were found to be in good agreement with previous measurements. The individual group yields reported here are preliminary and are being further refined.

INTRODUCTION

The long term toxicity of spent nuclear fuel, excluding plutonium, is dominated by the higher mass actinide isotopes, i.e., Np-237 and to a lesser extent Am-241, Am-243, and Cm-244.¹ The safe geological disposal of these isotopes with long-lived decay chains is difficult to prove. An alternative option to direct geological disposal is to remove the higher actinides from the spent fuel by chemical means, to load them into new fuel elements, and to transmute them by neutron induced fission into shorter-lived fission fragments. Reactors designed to transmute actinide waste isotopes are called actinide burner reactors.

The higher actinides are produced from successive radiative capture reactions starting with the U-238 in the reactor fuel. From an analysis of the fission and radiative capture cross-sections for the waste actinides (see Fig. 1 for cross-sections for Np-237), it can be observed that the fission-to-capture ratio increases dramatically at high neutron energies (i.e. above 100 keV). Therefore, to effectively transmute the waste isotopes while decreasing the production of more actinides, burner reactors are favored that operate with a fast or at least intermediate energy neutron flux spectrum. In order to effectively operate actinide burner reactors with large loadings of higher actinide isotopes in their cores, accurate knowledge of each actinide isotope's neutronic properties (including its delayed neutron properties) is important.

"The submitted manuscript has been authored by a contractor of the U.S. Government under contract No. DE-AC05-96OR22464. Accordingly, the U.S. Government retains a nonexclusive royalty-free license to publish or reproduce the published form of this contribution, or allow others to do so, for U.S. Government purposes."

DISTRIBUTION OF THIS DOCUMENT IS UNLIMITED

MASTER

DISCLAIMER

Portions of this document may be illegible in electronic image products. Images are produced from the best available original document.

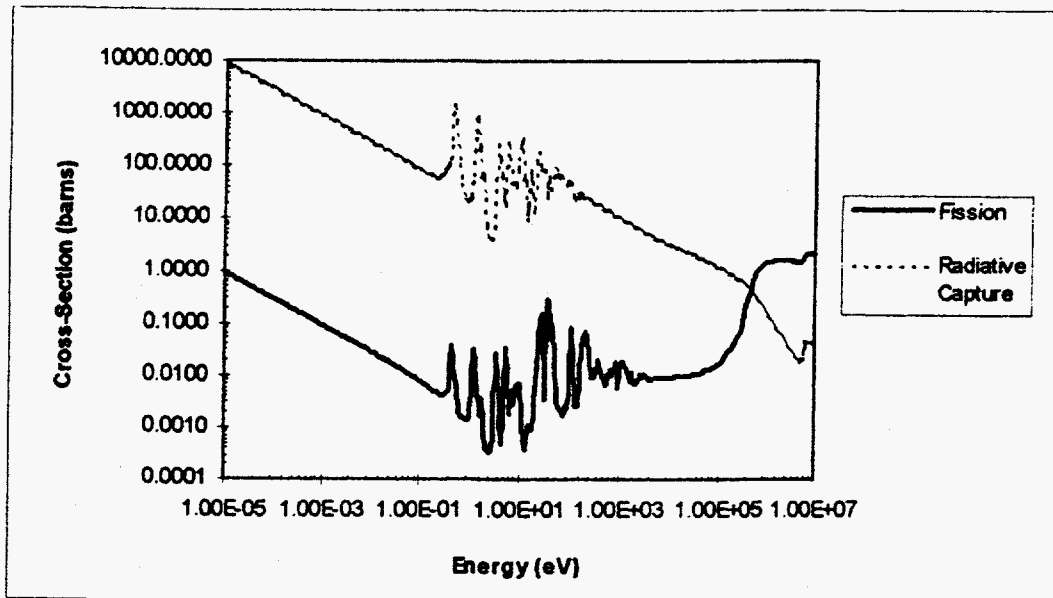


Fig. 1. Microscopic Interaction Cross-Sections (Fission and Radiative Capture) for Np-237.

While significant effort has been spent determining the delayed neutron emission properties of the higher actinides as a result of thermal neutron induced fission, comparatively less effort has been spent measuring these properties for fast fissioning systems.^{2,4} To supplement the existing neutronics database, an experiment at the Texas A&M University Nuclear Science Center (NSC) was conducted to measure the time-dependent delayed neutron yields of U-235 and Np-237 as a result of fast fission. The Nuclear Science Center Reactor (NSCR) is a 1 MW pool-type TRIGA reactor using FLIP fuel. This reactor operates with a predominately thermal neutron flux spectrum. Therefore, a specialized device using a B₄C filter was designed, built, installed, and characterized to achieve an in-core fast neutron flux irradiation capability.

EXPERIMENTAL DESIGN

The measurement technique used in these experiments was similar to that adopted by Keepin *et al.*³ To perform the delayed neutron measurements, several components had to be designed and constructed at the NSC. These systems included the in-core (fast neutron) irradiation device, a quick pneumatic transfer system, a detector array, photosensors, and an integrated computer control module. The entire system, including pneumatic transfers and detector counting, was controlled by a computer system with an internal I/O board. The system was designed to automatically perform the functions that follow: (1) the sample was transferred into the core when prompted, (2) the sample was allowed to irradiate for a preselected time period, (3) the sample was transferred to a BF₃ detector array where the counts versus time after irradiation were collected, and (4) the sample was transferred to a remote storage location. To minimize the sample transit time from core to detector, the detector array was located at the reactor bridge level. A sample transit time of 0.52 seconds was achieved from the irradiation position to the counting position.

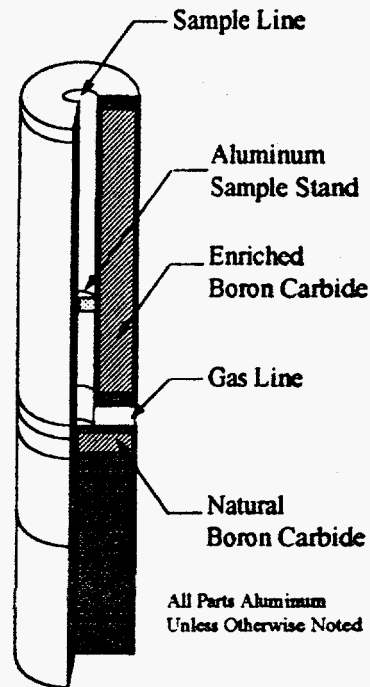


Fig. 2. *Fast Flux Pneumatic Receiver (Cross-sectional View, Shroud not Shown).*

Two U-235 and two Np-237 sources (fabricated by Isotope Products Laboratory in California) were used during the irradiations. The samples contained 11.95 mg and 12.27 mg of uranium (in a pressed oxide) and 9.79 mg and 10.27 mg of neptunium (in a pressed oxide), respectively. The uranium sources contained 97.663 atomic percent U-235, and the neptunium sources contained 99.23 atomic percent Np-237. Each sample (referred to as a rabbit) was double encapsulated in heat-sealed, low-density polyethylene vials. This procedure protected the pneumatic and detector systems against contamination.

Fast Flux Irradiation Device

The irradiation device, called the Fast Flux Pneumatic Receiver (FFPR), consists of twelve individually machined aluminum parts welded together with a sheath of 0.5" thick highly enriched boron carbide (90% ^{10}B by weight) that encompasses the position containing the actinide sample during irradiation (see Fig. 2 for a cross-sectional view of the internals of the FFPR). To decrease the number of thermal neutrons in the device due to streaming from below, a 0.5" thick plug of natural boron carbide is located near the inlet of the gas line. The device allows for pneumatic transfer of the rabbits to a perforated aluminum sample stand within the FFPR. The sample can be irradiated for a set period of time and then returned through the same sample line by supplying gas through the gas line. Due to the FFPR's voracious appetite for thermal neutrons, it has a reactivity worth of \$1.45. To facilitate submergence of the device in the reactor pool, it is weighted down by lead included in the grid plug at the base of the assembly. The entire receiver is enclosed in an aluminum square shroud (or box) which is used as a positioning aid when installing the device within the NSCR core. Note that the square shroud is not shown in Fig. 2.

The energy-dependent neutron flux spectrum within the FFPR was characterized using a foil activation technique. Eleven foils, both bare and cadmium covered (i.e. 22 samples total), were selected to provide a wide range of energy sensitivity. A list of the elements used, the reactions utilized, and the energy ranges of interest for each reaction are presented in Table I. Each foil was irradiated within the FFPR for 60 seconds. Gamma spectroscopy was used to determine the activity of the foils at the end-of-irradiation (EOI). These EOI activities were converted to saturation activities and provided as input along with a calculated initial "guess" to the spectrum unfolding code SAND-II. SAND-II was then run on a Sun SPARC-II to determine the neutron flux spectrum. SAND-II uses an iterative procedure to determine the energy-dependent neutron flux at 641 energy points spanning from 0.00001 eV to 20 MeV.

The $^{10}\text{B}(n,\alpha)^6\text{Li}$ reaction in the FFPR filter is exothermic and generates heat within the FFPR. The FFPR is not capable of transferring this heat to the pool water fast enough to maintain the FFPR walls near the pool water temperature during long irradiations. In order to prevent damage to the polyethylene rabbits due to high temperatures, the limiting irradiation time needed to be found. The irradiation time limit was determined by successive irradiations in which rabbit temperatures were measured. A maximum irradiation time of 60 seconds was found to be acceptable and it was used as the limit for all of the polyethylene encapsulated actinide samples. Aluminum sample holders (rabbits) were also designed and built which allowed for irradiation times of up to 10 minutes, but these were not used in obtaining the experimental results reported in this paper.

TABLE I
Flux Monitors Used to Characterize the FFPR Sample Region.

Element	Target	Reaction	Product	Half-life (hours)	Energy	Cross-Section (barns)
Ag	Ag-109	(n, γ)	Ag-110M	5995.2	4.47 eV	1689
Al	Al-27	(n, α)	Na-24	14.96	7.2 MeV	0.693
Au	Au-197	(n, γ)	Au-198	64.66	4.91 eV	1565
Co	Co-59	(n, γ)	Co-60	46165.8	132 eV	77
	Co-59	(n,p)	Fe-59	1068.0	6.8 MeV	0.143
Cu	Cu-63	(n, γ)	Cu-64	12.7	580 eV	5.6
Fe	Fe-54	(n,p)	Mn-54	7488.0	3.1 MeV	78
	Fe-58	(n, γ)	Fe-59	1068.0	230 eV	1.58
In	In-115	(n, γ)	In-116M	0.903	1.41 eV	3416
	In-115	(n,n')	In-115M	4.486	4.0 MeV	1.6
Mn	Mn-55	(n,2n)	Mn-54	7488.0	11.6 MeV	11.6
Ni	Ni-58	(n,p)	Co-58	1701.6	2.8 MeV	109
Ti	Ti-46	(n,p)	Sc-46	2011.4	3.9 MeV	10
	Ti-47	(n,p)	Sc-47	80.4	2.2 MeV	21.4
	Ti-48	(n,p)	Sc-48	43.7	7.6 MeV	0.303
Zn	Zn-64	(n,p)	Cu-64	12.7	2.8 MeV	30

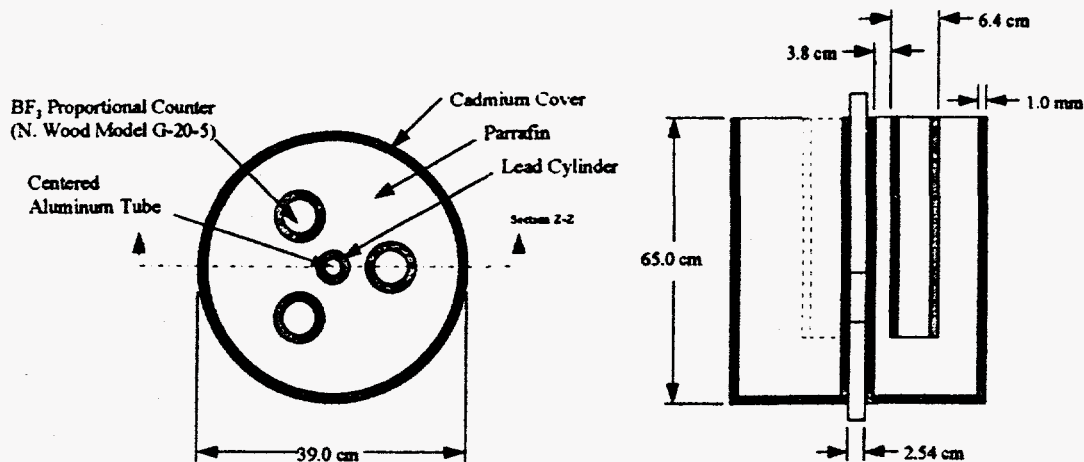


Fig. 3. *BF₃ Detector Array (Top and Longitudinal Cross-section Views).*

Detector Array and Electronics

A detector array consisting of three BF₃ tubes embedded in a polyethylene block (Fig. 3) was designed and built to allow for counting of the delayed neutrons emitted from the samples. The detector array has a 1" O.D. tube along its centerline in which the sample returning from the reactor is positioned. The gamma rays from the irradiated samples can interact in the BF₃ tubes and affect the recorded count rate. Thus a thin lead shield surrounded the sample tube in the polyethylene block to eliminate counts due to gamma ray pileup. A cadmium sheath also surrounds the outside of the block to absorb any extraneous or background sources of thermal neutrons (significant because the detector array is located at the reactor bridge level instead of in an isolated laboratory).

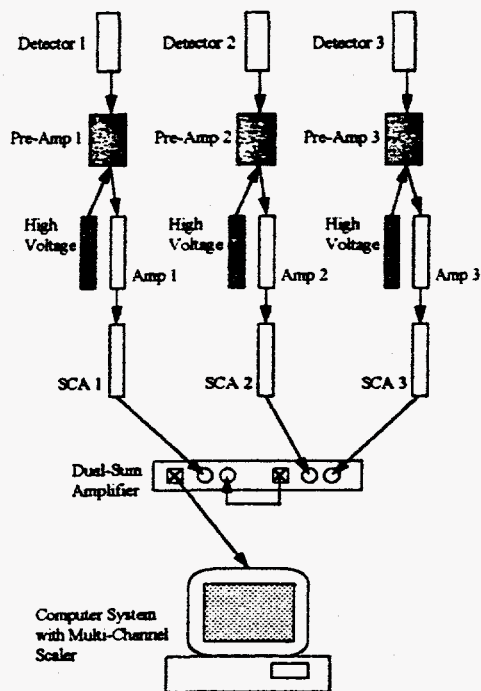


Fig. 4. *Detector Electronics Setup.*

The electronic components of the counting system are shown in Fig. 4. This system consisted of a series of BF₃ detectors attached to preamps, high voltage bias, amplifiers, and single channel analyzers. The individual signals from the three detectors are combined using a dual-sum inverting amplifier. The signal was then passed to a computer that allocated the pulses to various time bins. A 50.8 nCi Cf-252 source was used to measure the detector system's efficiency. It was found to be $7.41 \pm 0.52 \%$.

Delayed Neutron Measurements

The actinide samples were transferred into the reactor using a specially designed high speed pneumatically driven system (Fig. 5). This system was designed and constructed at the NSC using 1" O.D. polyethylene tubing and two unique passive divertors, machined and welded using stock aluminum, for enhanced sample transfer capabilities. The tubing and divertors were joined using Swagelok Unions. The high speed pneumatic system used CO₂ gas operating at 100 psi to propel the sample from the reactor to the detector following irradiation. The detectors were located at the reactor bridge level to minimize the rabbit's travel time from end of irradiation to the beginning of counting. A photosensor was located at the detector array. This sensor was used to measure a rabbit transit time of 0.52 seconds from core to detector. An integrated computer system was used to control the pneumatic transfer system and the detector arrays.

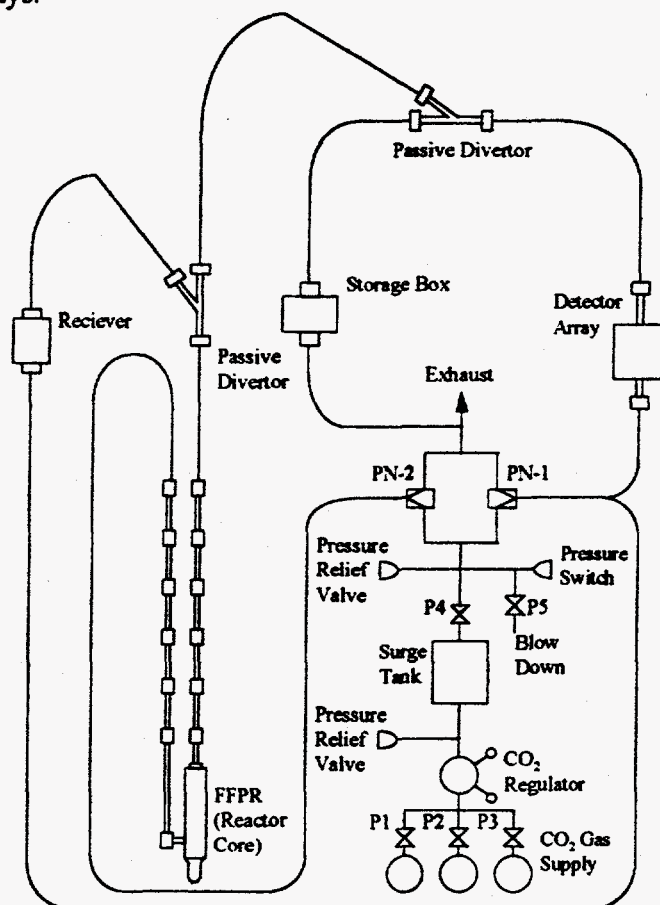


Fig. 5. Fast Pneumatic Transfer System Schematic.

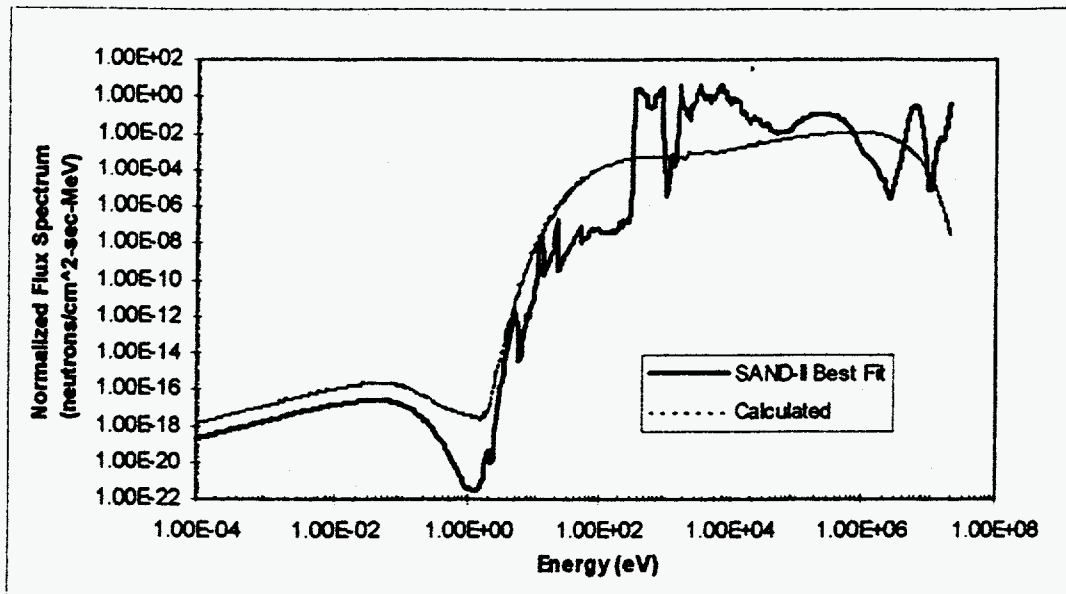


Fig. 5. Energy-Dependent Differential Neutron Flux in the FFPR at 1 MW (Calculated and SAND-II Best Fit Shown).

All of the samples were irradiated at 1 MW power, but different irradiation times (60.0, 20.0, and 5.0 seconds) and counting time increments (5.0, 1.0, and 0.1 seconds) were used to emphasize the importance of particular delayed neutron groups. After irradiation and counting, the samples were transferred to a storage box to allow for fission product decay prior to handling. After every irradiation, the fission rate was determined using a high purity germanium detector by measuring the activity of several fission products, in particular Ba-140, La-140, Ru-103, I-131, and Mo-99. The measured activities of Zr-99, Sr-91, Te-132, I-132, and I-135 (also fission products) were used as confirmatory information.⁷

RESULTS

Using the foil activation method and unfolding the acquired activities with the SAND-II unfolding code, a flux spectrum for the FFPR was determined. The spectrum unfolding code SAND-II requires an initial "guess" for the flux as input. To generate the initial flux, a Monte Carlo code was written for the FFPR. This code used the known external neutron flux (at the surface of the FFPR) as a source and calculated the flux within the FFPR using ENDF/B-V cross-section data. A plot of the calculated and the SAND-II results are presented in Fig. 5. Note the strong reduction in the portion of the neutron flux spectrum below ~50 eV.

The fission rate was determined for each sample after each irradiation. A decay period was allowed between irradiation and gamma-ray counting to allow for the shorter-lived fission products to decay. The fission rate was determined by a method similar to that used by Benedetti *et al.* using the measured activity of specific fission products.⁷

The delayed neutron curves were fit to five delayed neutron groups using the following relation:³

$$C(t) = R_f \cdot \epsilon \cdot \sum_i Y_i \cdot (1 - \exp(-\lambda_i \cdot t_{irr})) \cdot \exp(-\lambda_i \cdot t) \quad (1)$$

where $C'(t)$ is the count rate at time t following irradiation, R_f the fission rate, ϵ the detector efficiency, t_{ir} the irradiation time, and Y_i and λ_i the group yields and decay constants for the i^{th} group. The fit parameters for the U-235 and Np-237 samples are given in Tables II and III. The total yields per 100 fissions for U-235 and Np-237 were found to be 1.41 ± 0.09 and 1.02 ± 0.08 , respectively. In both of these calculations, contributions from the sixth group (half-life of 0.179 ± 0.017 seconds³) was neglected.

TABLE II
Delayed Neutron Yields and Decay Constants for U-235 (Comparison Data from Keepin et al. Provided).

Group	λ (s ⁻¹) (This Work)	Group Yield (%) (This Work)	λ (s ⁻¹) (Keepin et al.)	Group Yield (%) (Keepin et al.)
1	0.0127 ± 0.0003	0.070 ± 0.006	0.0127 ± 0.0002	0.063 ± 0.005
2	0.0322 ± 0.0011	0.335 ± 0.014	0.0317 ± 0.0008	0.351 ± 0.011
3	0.122 ± 0.002	0.331 ± 0.011	0.116 ± 0.003	0.310 ± 0.028
4	0.317 ± 0.009	0.468 ± 0.033	0.311 ± 0.008	0.672 ± 0.023
5	1.30 ± 0.10	0.209 ± 0.021	1.40 ± 0.08	0.211 ± 0.015

TABLE III
Delayed Neutron Yields and Decay Constants for Np-237 (Comparison Data from Benedetti et al. Provided).

Group	λ (s ⁻¹) (This Work)	Group Yield (%) (This Work)	λ (s ⁻¹) (Benedetti et al.)	Group Yield (%) (Benedetti et al.)
1	0.0142 ± 0.0008	0.217 ± 0.010	0.0127 ± 0.0002	0.0490 ± 0.0031
2	0.0322 ± 0.0007	0.229 ± 0.010	0.0318 ± 0.0006	0.310 ± 0.009
3	0.148 ± 0.002	0.261 ± 0.008	0.123 ± 0.002	0.251 ± 0.009
4	0.342 ± 0.006	0.215 ± 0.035	0.318 ± 0.004	0.454 ± 0.014
5	0.862 ± 0.160	0.119 ± 0.021	1.03 ± 0.17	0.129 ± 0.012

DISCUSSION

The flux spectrum determined using the flux monitors and unfolding code generally agrees with the calculated spectrum and shows that the thermal neutron flux is effectively suppressed. From an analysis of the flux and the fission cross-sections, it can be seen that the large resonances in most higher mass isotopes lie at energies between 10 eV and 100 eV. The FFPR flux decreases rapidly at energies less than 100 eV. In fact, the flux at 50 eV is seven orders of magnitude lower than the average flux between 1 keV and 10 MeV. This observation confirms that the flux used during the irradiations is dominated by the fast portion of the spectrum.

The delayed neutron yields and decay constants are slightly different than those calculated by Benedetti *et al.* and Keepin *et al.* Keepin³ reported a total yield per 100 fissions for U-235 of 1.61 ± 0.08 compared to our value of 1.41 ± 0.09 . Benedetti⁷ reported a total yield per 100 fissions for Np-237 of 1.03 ± 0.05 compared to our value of 1.02 ± 0.08 . The primary difference between these irradiations is in the purity of the samples used and the difference in the epithermal (100 eV to 1 keV) neutron flux in the FFPR compared to that of the Godiva reactor. The U-235 samples for these experiments were only 97.663% U-235. The remainder was composed primarily of U-234 (1.665%), U-236 (0.149%), and U-238 (0.519%). Thus, these impurities may have affected the overall accuracy of the U-235 yields. The Np-237 sample was extremely pure (99.23%) thus the yield data from these samples is virtually unaffected by the presence of impurities.

The transit time achieved using this system was slightly better than that achieved by Benedetti *et al.*, but was not as short as Keepin's. Thus, measurement of the sixth group (and shortest lived) was not possible. In order to generate an estimate of the sixth group to improve the comparison of the curve fits with that of other experimenters, the sixth group can be obtained from nuclear models.⁵ However, this has not been accomplished as of the time of writing.

The primary sources of error in the measured results are due to determination of the fission rate and the parameter fit. The error due to the counting statistics were generally quite small. The count rates acquired ranged from 40,000 cps to 1000 cps (after several minutes decay). The detector dead time (measured using the "two-source method") was determined to be $7.56 \pm 0.12 \mu\text{s}$. Thus, only slight correction was necessary to account for detector dead time. Measurement of the fission rate relied upon the accuracy of the fission product yields, and the short irradiations tended to yield small fission product quantities thus making very accurate determination difficult. The errors associated with the parameter fit was determined using the same procedure adopted by Keepin *et al.*³

The total delayed neutron yield for U-235 from fast neutron induced fission is significantly less than that found from thermal neutron induced fission. The total yield per 100 fissions for U-235 recommended by Waldo *et al.* is 1.654 ± 0.033 .⁶ This value is significantly higher than that determined here. For Np-237, the difference in the fast fission versus thermal fission total yields is much less than for U-235. Waldo *et al.* reported a value of 1.068 ± 0.098 delayed neutrons per 100 fissions for Np-237, which is only slightly larger than that determined here.⁶

CONCLUSIONS

The results acquired in these irradiations yielded generally good agreement with those obtained by Keepin *et al.* and Benedetti *et al.* However, the individual group yields and decay constants could not be compared directly as the transit time achieved does not allow identification of a full six delayed neutron groups. Further work needs to be performed to include the sixth group based on values from nuclear models. While measurement of the properties of the sixth group is beyond the capabilities of this system, errors in the properties of the fifth group may be decreased by increasing the pneumatic system gas pressure from 100 psi to 120 psi, thus decreasing the sample transit time.

The neutron flux spectrum measured in the FFPR is effectively free of contributions due to neutron energies below 50 eV. The FFPR will therefore be useful for other sample

irradiations in which it is desired to suppress thermal neutron induced radiative capture reactions. The system used here will also be used for delayed neutron measurements from Am-241 and Am-243 in the near future.

ACKNOWLEDGMENTS

The research presented here was funded under the auspices of the Japan/U.S. Actinide program of Oak Ridge National Laboratory (ORNL) in cooperation with collaborators at the Japan Atomic Energy Research Institute (JAERI). ORNL is operated by Lockheed Martin Energy Research Corporation under Contract No. DE-AC05-96OR22464 with the U.S. Department of Energy. The authors appreciate the interest in the development and improvement of nuclear data exhibited by T. Mukaiyama and H. Oigawa (JAERI)

REFERENCES

1. T. MUKAIYAMA, H. TAKANO, T. TAKIZUKA, T. OGAWA, and M. OSAKABE, "Conceptual Study of Actinide Burner Reactors," *Proceedings of the 1988 International Reactor Physics Conference*, Jackson Hole, Wyoming, Vol. IV, 369 (September 1988).
2. M. C. BRADY, R. Q. WRIGHT, and T. R. ENGLAND, "Actinide Nuclear Data for Reactor Physics Calculations," ORNL/CSD/TM-266, Oak Ridge National Laboratory, Oak Ridge, Tennessee (1991).
3. G. R. KEEPIN, T. F. WIMETT, and R. K. ZEIGLER, "Delayed Neutrons from Fissionable Isotopes of Uranium, Plutonium, and Thorium," *J. Nucl. Energy*, **6**, 1-21 (1957).
4. G. R. KEEPIN, T. F. WIMETT, and R. K. ZEIGLER, "Delayed Neutrons from Fissionable Isotopes of Uranium, Plutonium, and Thorium," *Phys. Rev.*, **107**, 1044-49 (1957).
5. R. J. TUTTLE, "Delayed Neutron Data for Reactor Physics Analysis," *Nucl. Sci. and Eng.*, **56**, 37 (1975).
6. R. W. WALDO, R. A. KARAM, and R. A. MEYER, "Delayed Neutron Yields: Time Dependent Measurements and a Predictive Model," *Phys. Rev. C*, **23**, 1113 (1981).
7. G. BENEDETTI, A. CESANA, V. SANGUIST, M. TERRANI, and G. SANDRELLI, "Delayed Neutron Yields from Fission of U-233, Np-237, Pu-238, Pu-240, Pu-241, and Am-241," *Nucl. Sci. and Eng.*, **80**, 379-87 (1982).
8. S. A. COX, "Delayed-Neutron Studies from the Thermal-Neutron-Induced Fission of Pu-241," *Phys. Rev.*, **123**, 1735-39 (1961).

DISCLAIMER

This report was prepared as an account of work sponsored by an agency of the United States Government. Neither the United States Government nor any agency thereof, nor any of their employees, makes any warranty, express or implied, or assumes any legal liability or responsibility for the accuracy, completeness, or usefulness of any information, apparatus, product, or process disclosed, or represents that its use would not infringe privately owned rights. Reference herein to any specific commercial product, process, or service by trade name, trademark, manufacturer, or otherwise does not necessarily constitute or imply its endorsement, recommendation, or favoring by the United States Government or any agency thereof. The views and opinions of authors expressed herein do not necessarily state or reflect those of the United States Government or any agency thereof.